

# Model-Free Power System Stability Enhancement with Dissipativity-Based Neural Control

Yifei Wang\*, Han Wang\*, Kehao Zhuang†, Keith Moffat‡ and Florian Dörfler\*

\* Automatic Control Laboratory, ETH Zurich, Zurich

† College of Electrical Engineering, Zhejiang University, Hangzhou, China

‡ Department of Electrical and Electronic Engineering, The University of Melbourne, Melbourne, Australia

{wangyife, hanwang1, dorfler}@ethz.ch, keith.moffat@unimelb.edu.au, zhuangkh@zju.edu.cn

**Abstract**—The integration of converter-interfaced generation introduces new transient stability challenges to modern power systems. Classical Lyapunov- and scalable passivity-based approaches typically rely on restrictive assumptions, and finding storage functions for large grids is generally considered intractable. Furthermore, most methods require an accurate grid dynamics model. To address these challenges, we propose a model-free, nonlinear, and dissipativity-based controller which, when applied to grid-connected virtual synchronous generators (VSGs), enhances power system transient stability. Using input-state data, we train neural networks to learn dissipativity-characterizing matrices that yield stabilizing controllers. Furthermore, we incorporate cost function shaping to improve the performance with respect to the user-specified objectives. Numerical results on a modified, all-VSG Kundur two-area power system validate the effectiveness of the proposed approach.

**Index Terms**—Dissipativity, Lyapunov stability, Neural networks, Transient stability, Virtual synchronous generators

## I. INTRODUCTION

Modern power systems are undergoing significant transformations with the increasing penetration of renewable energy [1]. Renewable resources such as wind and solar power are interfaced with the grid through power electronics converters. These converters can be controlled to behave as virtual synchronous generators (VSGs) that emulate traditional synchronous generators (SGs) in either grid-forming or grid-following mode [2]. Conventional SG control schemes, constrained by the physical limitations of the SG, are inflexible and can be ineffective for grid stabilization challenges such as subsynchronous oscillation damping [3]. This is particularly true for low-inertia grids [4]. In contrast to SGs, converters are flexible and many more advanced control structures [5]–[8] have been developed.

Traditionally, power system transient stability analysis and subsequent control design have been based on (or have aspired to using) Lyapunov's direct method [9], [10]. However, analytically finding Lyapunov or energy functions is often challenging, as the derivation is often highly model-specific and can suffer from the lack of a systematic methodology [11]. Moreover, the problem remains unsolved even for simple

system models if certain unrealistic assumptions, such as the lossless property of the system, are relaxed [11], [12]. Studies [12]–[15] have employed passivity theory to perform stability analysis or to design the control and the Lyapunov function simultaneously. However, restrictive assumptions are still required for passivity to hold. As the complexity of power systems increases, it is advantageous to directly investigate *dissipativity*, which is a generalization of passivity [16]. For example, the studies [17], [18] present dissipativity-based control of DC microgrids. Nevertheless, extensions to nonlinear, AC power system applications, such as the transient angle stability of VSGs, remain largely unexplored.

Dissipativity-based control requires the design of storage and supply rate functions, which are difficult for nonlinear power system even when the dynamics are known. Current literature mainly considers the special case of Lyapunov or energy functions, but can provide heuristics for dissipativity characterization. To overcome the difficulty of finding analytical expressions discussed previously, studies have used numerical techniques such as linear matrix inequalities [19] or sum of squares programming [11] to provide more general frameworks for Lyapunov function design, but these methods are still constrained by the expressivity of the chosen parametrization. Alternatively, studies have taken advantage of neural network (NN) expressivity to learn Lyapunov functions [20] and to find larger stability regions for power systems [21]–[23]. However, the use of NNs to characterize dissipativity has received limited attention.

In addition to the challenge of finding dissipativity-characterizing functions, power system engineers also face model-accuracy challenges. One option is to use NNs to learn the dynamics before learning the storage function (or the Lyapunov or energy function) [24]. However, such a two-stage learning procedure may suffer from error accumulation. This motivates our data-driven approach, which *learns the dissipative properties directly from the data*.

The main contributions of this work are as follows. We develop a novel method that directly learns the dissipativity of VSG-based power systems with properly designed neural networks, which output general, symmetric, or symmetric positive definite matrices. We introduce loss functions corresponding to violations of dissipativity and stability conditions so that the matrix NNs compose a stabilizing control for the

Submitted to the 24th Power Systems Computation Conference (PSCC 2026).

system. Using the extra degrees of freedom in the dissipativity condition, we also add cost function shaping to enhance the optimality of our control with respect to user-defined performance metrics. Finally, we conduct numerical transient stability experiments on a single converter infinite bus (SCIB) system and the modified Kunder two-area system with four VSGs, demonstrating the effectiveness of our approach.

This paper is organized as follows. Section II introduces the background knowledge. Section III presents our dissipativity-based neural control. Section IV presents the numerical experiments. Section V concludes the paper.

## II. PRELIMINARIES

This section introduces preliminary knowledge that supports our control design.

### A. Power System Transient Stability

In transient analysis of converter-interfaced power systems, it is common to ignore the faster inner-loop dynamics and to use a lower-order model, such as the following second-order swing equation in a VSG-controlled system

$$\begin{cases} M_i \frac{d\omega_i}{dt} = P_{\text{ref},i} - P_{\text{e},i}(\delta) - D_i(\omega_i - 1) + u_i \\ \frac{d\delta_i}{dt} = \omega_B(\omega_i - 1) \end{cases} \quad (1)$$

for VSG at bus  $i \in \{1, 2, \dots, N\}$ , where  $M_i$ ,  $P_{\text{ref},i}$ ,  $D_i$ ,  $\omega_i$ , and  $\delta_i$  are the moment of inertia (in s), the power reference (p.u.), the damping coefficient (p.u.), the angular frequency (p.u.), and the relative power angle (rad) with respect to a synchronous reference frame, and  $\omega_B$  is the base (nominal) frequency in rad/s. A control input  $u_i$  can be additionally added to the frequency dynamics of the  $i$ -th VSG. The electrical power output of converter  $i$  is

$$P_{\text{e},i} = E_i^2 G_{ii} + \sum_{\substack{j=1 \\ j \neq i}}^N E_i E_j [G_{ij} \cos(\delta_{ij}) + B_{ij} \sin(\delta_{ij})],$$

where  $E_i$  is the virtual electromotive force of the  $i$ -th VSG determined by state variables,  $\delta_{ij} = \delta_i - \delta_j$  represents power angle difference, and  $G_{ij}$  and  $B_{ij}$  are the conductance and susceptance elements of the reduced network admittance matrix between VSG  $i$  and  $j$  after Kron reduction.

Compactly, the dynamics of the power system are described by a set of continuous-time differential equations. However, as VSG controllers are digital and due to the data-driven requirement that data can only be sampled at discrete times, we should consider discrete-time dynamics. Assuming a constant sampling and control interval  $\Delta t$  and corresponding zero-order-hold inputs, the continuous dynamics can be described at sampling instants by the following difference equation:

$$x_{k+1} = f(x_k, u_k), \quad (2)$$

where, more generally,  $x_k \in \mathcal{X} \subset \mathbb{R}^n$  and  $u_k \in \mathcal{U} \subset \mathbb{R}^m$  are the states and inputs defined over a compact set  $\mathcal{X} \times \mathcal{U}$ ; the nonnegative integer  $k$  is the discrete time step;  $f : \mathcal{X} \times$

$\mathcal{U} \rightarrow \mathbb{R}^n$  is locally Lipschitz continuous on  $\mathcal{X} \times \mathcal{U}$ . When  $u$  becomes a function of  $x$  through a locally Lipschitz continuous feedback control law  $u_k = \pi(x_k)$ ,  $\pi : \mathcal{X} \rightarrow \mathcal{U}_\pi \subseteq \mathcal{U}$ , the closed-loop system becomes autonomous:

$$x_k = f(x_k, \pi(x_k)) = f_\pi(x_k). \quad (3)$$

The local asymptotic stability of (3) is defined as follows.

**Definition 1:** Suppose  $x^*$  is an equilibrium point of (3), i.e.  $f_\pi(x^*) = 0$ , then the system is *stable* with respect to  $x^*$  if  $\forall \varepsilon > 0, \exists \delta > 0$ , such that  $\|x_0 - x^*\| < \delta \Rightarrow \forall k \geq 0, \|x_k - x^*\| < \varepsilon$ . Further, it is *(locally) asymptotically stable* if  $\exists \delta' > 0$ , such that  $\|x_0 - x^*\| < \delta' \Rightarrow \lim_{k \rightarrow \infty} \|x_k - x^*\| = 0$ . The set that contains all  $x'$  such that  $x_0 = x' \Rightarrow \lim_{k \rightarrow \infty} x(t) = x^*$  is termed as the *region of attraction* (RoA) of  $x^*$ .

Classical transient stability analysis in power systems seeks to determine whether the system states, after a large disturbance such as a fault, are in the RoA of the (locally) stable post-fault equilibrium. With appropriate control, the RoA of the post-fault equilibrium can be enlarged and the transient stability can be improved.

### B. Lyapunov Function and Dissipativity

Without loss of generality, we assume  $f(0, 0) = 0$  in (2) and  $\pi(0) = 0$ , which leads to  $f_\pi(0) = 0$  in (3).

In the controlled system (3), the asymptotic stability with respective to  $x^* = 0$  is established by the following Theorem.

**Theorem 1** ([25, Exercise 4.63]): The equilibrium  $x^* = 0$  of (3) is asymptotically stable if there exists a compact and non-empty set  $D \subseteq \mathcal{X}$  that includes the origin, and there is a function  $V : D \rightarrow \mathbb{R}$ , termed *Lyapunov function*, that satisfies

$$\begin{aligned} V(x_k) &> 0, \quad x_k \in D \setminus \{0\}, \quad V(0) = 0, \\ V(x_{k+1}) - V(x_k) &< 0, \quad x_k \in D \setminus \{0\}. \end{aligned} \quad (4)$$

Theorem 1 is commonly used as a powerful method in analyzing the stability of autonomous systems, while in the analysis of open-loop systems with external inputs, dissipativity has been proposed as a generalization of Lyapunov stability.

**Definition 2** (Dissipativity): System (2) is *locally dissipative with respect to a supply rate function*  $w(\cdot, \cdot) : \mathcal{X} \times \mathcal{U} \rightarrow \mathbb{R}$  if there exist a *storage function*  $V : \mathcal{X} \rightarrow \mathbb{R}$  and compact and non-empty sets  $D_x \subseteq \mathcal{X}$ ,  $D_u \subseteq \mathcal{U}$  containing the origins such that along system trajectories

$$V(x_k) \geq 0, \quad x_k \in D_x \setminus \{0\}, \quad V(0) = 0, \quad (5a)$$

$$V(x_{k+1}) - V(x_k) \leq w(x_k, u_k), \quad \forall x_k \in D_x, u_k \in D_u. \quad (5b)$$

Here, the supply rate is a function of states  $x_k$  and inputs  $u_k$  instead of the more common choice of outputs  $y_k$  and  $u_k$ . The left-hand side of (5b) can be interpreted as the rate of change of the stored energy of the system, which should be smaller than the energy supply rate on the right-hand side if the system is dissipative with respect to the supply rate. This property naturally reminds us of the dissipative characteristics of a real-world power system.

In addition to designing arbitrary controllers that maintain the stability of the operating equilibrium and further enhance

the transient stability VSGs, we often desire an optimal one with respect to certain performance criteria, such as minimizing the frequency deviation during the transients. A general optimal control problem with an asymptotic stability requirement is given as follows:

$$\begin{aligned} \min_{\{u_k\}_{k=0}^{\infty}} \quad & \sum_{k=0}^{\infty} l(x_k, u_k) \\ \text{subject to} \quad & x_{k+1} = f(x_k, u_k), \quad x_0 \text{ given} \\ & \lim_{k \rightarrow \infty} x_k = 0. \end{aligned} \quad (6)$$

where  $l(\cdot, \cdot) : \mathcal{X} \times \mathcal{U} \rightarrow \mathbb{R}_+$  is a nonnegative real cost function. A solution to (6) is referred to as an *optimal stabilizing control*.

### III. METHODOLOGY

In this section, we illustrate our data-driven neural controller design method to enhance the stability of dissipative VSG-based power systems with unknown dynamics. We first introduce a dissipativity-based control and conditions that make it a stabilizing one. We then demonstrate how to use NNs to find storage and supply rate functions that characterize the dissipativity of unknown power systems, as well as to synthesize stabilizing controllers.

#### A. Dissipativity-Based Stabilizing Control

Studies have proposed stabilizing feedback controllers for dissipative systems. Inspired by existing static feedback controls [26], [27] and continuous-time dynamic feedback control [28], we propose a dynamic feedback control for discrete-time settings as required by the data-driven context.

Without loss of generality, we assume  $f(0, 0) = 0$  in the following analysis. By comparing the dissipativity conditions (5a)-(5b) with those stated in (4), it follows that if

$$\pi(0) = 0, \quad w(x, \pi(x)) < 0, \quad \forall x \in D/\{0\} \quad (7)$$

and the system is dissipative with respect to  $w$  with a positive definite storage function  $V$ ,  $\pi(x)$  will stabilize the system toward the origin. To this end, we have the following theorem.

**Theorem 2:** Suppose that system (2) is dissipative on  $D_x = \mathcal{X}$ ,  $D_u = \mathcal{U}$  with respect to generalized  $(Q, S, R)$  supply rate

$$w(x, u) = x^T Q(x) x + 2x^T S(x) u + u^T R(x) u \quad (8)$$

with  $Q^T(\cdot) = Q(\cdot) : \mathcal{X} \rightarrow \mathbb{R}^{n \times n}$ ,  $S(\cdot) : \mathcal{X} \rightarrow \mathbb{R}^{n \times m}$ ,  $0 \prec R(\cdot) : \mathcal{X} \rightarrow \mathbb{R}^{m \times m}$ , and a positive definite storage function  $V(x)$ . If

$$\Delta(x) := S(x)R^{-1}(x)S^T(x) - Q(x) \succ 0, \quad \forall x \in \mathcal{X} \quad (9)$$

holds, and the range of control

$$\pi(x) = -R^{-1}(x)S^T(x)x \quad (10)$$

is a subset of  $\mathcal{U}$ , then (7) always holds with control (10) and supply rate (8). Moreover, (10) is a stabilizing control.

**Proof:** The proof is given in Appendix A.

Theorem 2 provides us with insights on how to design stabilizing controls based on dissipativity. A natural interpretation is that the control should supply as little energy as possible

to the system. To see this, consider constant  $Q$ ,  $S$ , and  $R$ , then the supply rate becomes  $u^T Ru + 2x^T Su + x^T Qx$ , a quadratic function of  $u$ . With  $R$  positive definite, the function is minimized when  $u = -R^{-1}S^T x$  and the minimum value is exactly  $-x^T \Delta(x)x$ . Therefore, we obtain a low upper bound for the increase in the storage function  $V$  in one time step. If additionally such an upper bound is negative definite,  $V$  can only be strictly decreasing unless it reaches  $V = 0$ , bringing the system to equilibrium. The minimization of the supply rate function implies the infinite-horizon optimality of the proposed dissipativity-based control, as shown in the following theorem.

**Theorem 3:** Suppose that system (2) satisfies all the conditions of Theorem 2, then the control (10) is the solution to the following optimal control problem:

$$\begin{aligned} \min_{\{u_k\}_{k=0}^{\infty}} \quad & \sum_{k=0}^{\infty} [\tilde{l}(x_k, u_k) + x_k^T \Delta(x_k) x_k] \\ \text{subject to} \quad & x_{k+1} = f(x_k, u_k), \quad x_0 \text{ given} \\ & \lim_{k \rightarrow \infty} x_k = 0, \end{aligned} \quad (11)$$

where  $\tilde{l}(x_k, u_k) = -[V(x_{k+1}) - V(x_k)] + w(x_k, u_k)$  is a nonnegative cost function, and  $x_k^T \Delta(x_k) x_k$  is positive definite.

**Proof:** The proof is given in Appendix B.

Although (11) involves the system dynamics  $x_{k+1} = f(x_k, u_k)$ , this merely reflects that the costs are evaluated along system trajectories. Theorem 3 emphasizes the inherent optimality of (10) consistent with the dissipative property, while not relying on explicit knowledge of the dynamic model.

#### B. The Matrix Neural Networks

In order to generate a stabilizing control according to Theorem 2, the functions  $V(x)$ ,  $Q(x)$ ,  $S(x)$ , and  $R(x)$  satisfying the theorem's conditions are required. Even for a power system with known dynamics, finding such functions would be challenging. Furthermore, an accurate system model is not always available. Therefore, we leverage data and the function approximation ability of NNs to directly learn functions that satisfy conditions in Theorem 2. Certain conditions can be satisfied by appropriate NN architectures, while others are results of NN training driven by corresponding loss functions. For simplicity, we use relative states with respect to the equilibrium of the specific post-fault system in the concerned transient stability case, and the origin in the new coordinates therefore becomes an equilibrium point.

To begin with, we have the following parameterizations:

- $V(x; \theta_W) = x^T W(x; \theta_W) x$  with an  $n \times n$  positive definite matrix NN  $W(x; \theta_W)$  is positive definite;
- an  $n \times n$  symmetric matrix NN  $Q(x; \theta_Q)$ ;
- an  $n \times m$  matrix NN  $S(x; \theta_S)$ ;
- an  $m \times m$  positive definite matrix NN  $R^{-1}(x; \theta_{R^{-1}})$  whose inverse is  $R(x; \theta_{R^{-1}})$ ,

where  $\theta$  represents the NN parameters. We use three types of matrix NNs that are built as follows:

- An (ordinary) matrix NN with dimension  $p \times q$  is obtained by reshaping the output of a multilayer perceptron (MLP) with  $n$  input units and  $pq$  output units as a  $p \times q$  matrix;

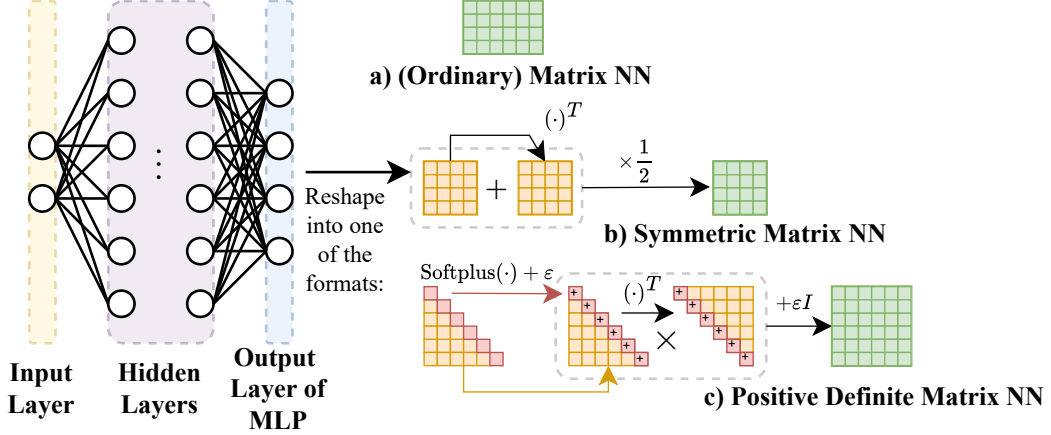


Fig. 1. The architecture of three types of matrix NNs. For simplicity, we only draw one MLP schematic. Different matrix NNs do not share the same MLP.

- A symmetric matrix NN with dimension  $p \times p$  is obtained by averaging the output of an ordinary  $p \times p$  matrix NN with its transpose;
- To obtain a  $p \times p$  positive definite matrix NN, we reshape the output of an MLP with  $n$  input units and  $p(p + 1)/2$  output units as a lower triangular matrix  $L$ , pass the diagonal elements to the softplus function  $\text{Softplus}(x) = \ln(1 + \exp(x)) > 0$ , add a small  $\varepsilon > 0$  to them, and keep the non-diagonal entries to obtain  $\tilde{L}$ , compute  $\tilde{L}\tilde{L}^T$ , and finally add another small  $\varepsilon > 0$  to the diagonal elements. The positive definiteness of the output is governed by the Cholesky decomposition form. The small  $\varepsilon > 0$  slightly restricts the approximation ability of the NN, but is beneficial in terms of numerical stability. Additionally, we allow this type of NN to output its inverse, as seen in the case of  $R^{-1}(x; \theta_{R^{-1}})$ .

Figure 1 summarizes the architectures of the matrix NNs we use.

### C. Loss Function Design

After building the matrix NNs, we define loss functions that penalize the violations of conditions of Theorem 2.

According to the dissipativity condition (5b) with supply rate (8), we define the following loss function that penalizes the violation of the dissipativity conditions:

$$\begin{aligned} \mathcal{L}_d(\theta, \mathcal{B}) &:= \max_{d_k \in \mathcal{B}} \text{Softplus}(\varepsilon_d + x_{k+1}^T W(x_{k+1}; \theta_W) x_{k+1} \\ &\quad - x_k^T W(x_k; \theta_W) x_k - x_k^T Q(x_k; \theta_Q) x_k - 2x_k^T S(x_k; \theta_S) u_k - u_k^T R(x_k; \theta_{R^{-1}}) u_k) \\ &:= \max_{d_k \in \mathcal{B}} \text{Softplus}(\varepsilon_d + (*)), \end{aligned} \quad (12)$$

where  $\theta$  refers to all the NN parameters,  $(*)$  is the violation of the dissipativity condition,  $\varepsilon_d > 0$  is a small margin that encourages the violation to be smaller and provides more safety, and  $\mathcal{B}$  is a batch of data tuples  $d_k = (x_k, x_{k+1}, u_k)$ . We use the softplus function because it is smooth and its gradient does not disappear when the input is non-positive. We use the maximum loss within a batch instead of the usual average

loss because we want a conservative result where the largest violation should be non-positive.

Next, the loss corresponding to stability condition (9) is:

$$\mathcal{L}_\Delta(\theta; \mathcal{B}) := \max_{d_k \in \mathcal{B}} \text{Softplus}(\varepsilon_\Delta - \min \text{eig}(\Delta(x_k; \theta))), \quad (13)$$

where  $\varepsilon_\Delta > 0$  is again a small margin that encourages larger minimum eigenvalues, and  $\min \text{eig}(\cdot)$  computes the smallest eigenvalue of the input. Therefore, (13) punishes the smallest negative eigenvalue of  $\Delta(x_k)$ , driving it positive definite.

To utilize Theorem 3 and optimize long-term performance on top of stability, we compare (6) and (11) and find it beneficial to let  $\bar{l}(x, u) + x^T \Delta(x) x + u^T R(x) u$  be equal to a user-defined cost  $l(x, u)$ . Therefore, we define the following cost shaping loss function:

$$\mathcal{L}_{sp}(\theta; \mathcal{B}) = \frac{1}{|\mathcal{B}|} \left[ \frac{l(x_k, u_k) - (x_k^T \Delta(x_k; \theta) x_k - (*))}{|l(x_k, u_k)| + \varepsilon_{sp}} \right]^2, \quad (14)$$

where  $(*)$  is defined as in  $\mathcal{L}_d$ , and  $l(x, u)$  is a user-defined positive definite cost. We use the relative error and a small margin  $\varepsilon_{sp} > 0$  to enhance the numerical stability.

In addition, we add a regularization term  $\mathcal{L}_r(\theta)$  that penalizes the  $\ell^1$  norm of the NN parameters. This term helps prevent parameters from becoming too large, promotes sparsity, and enhances numerical stability. The total batch loss is then

$$\mathcal{L}(\theta, \mathcal{B}) = w_1 \mathcal{L}_d(\theta, \mathcal{B}) + w_2 \mathcal{L}_\Delta(\theta, \mathcal{B}) + w_3 \mathcal{L}_{sp}(\theta, \mathcal{B}) + w_4 \mathcal{L}_r(\theta), \quad (15)$$

where  $w_1 > 0$ ,  $w_2 > 0$ ,  $w_3 \geq 0$ ,  $w_4 \geq 0$  are tunable weights.

### D. Learning Dissipativity with Neural Networks

With the defined matrix NNs and the loss functions, we use the usual neural network training workflow to train our matrix NNs. To begin with, we sample states and inputs from the trajectories of the specific unknown (post-fault) system and rearrange them into a data set  $\mathcal{D}$  in the form of  $\{(x_k, x_{k+1}, u_k)\}_{k=1}^M$  for convenience, where  $M$  is the total number of tuples. We set the number of epochs and divide  $\mathcal{D}$  into batches in each epoch. For each batch, we calculate the loss (15) and update the NN parameters with

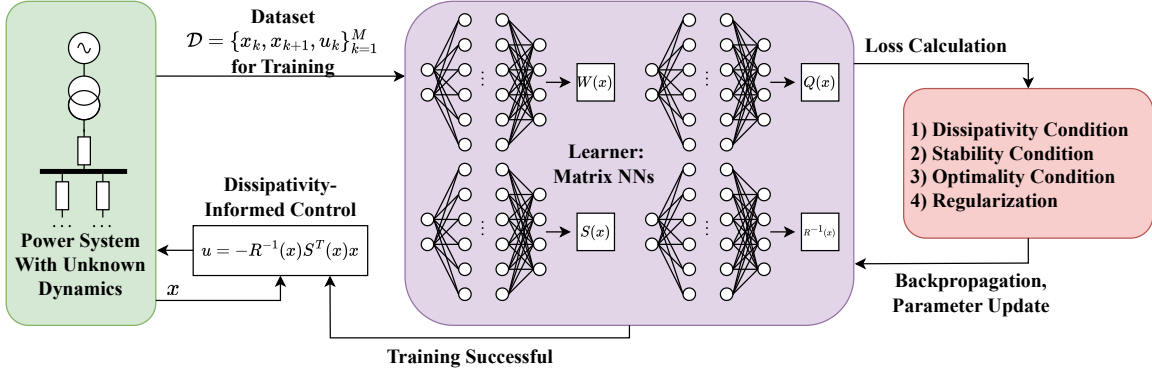


Fig. 2. An overview of our algorithm, which generate a stabilizing control after training NNs that can characterize dissipativity.

the Adam optimizer, a highly efficient first-order optimization algorithm [29]. When training is complete, the NNs generate a control  $\pi(x)$  according to (10). The effectiveness of the algorithm is dependent on the richness of the training data. Therefore, we have to implement the returned control law  $\pi(x)$  to see if it indeed stabilizes the closed-loop system. Tuning of the hyperparameters is often necessary. Since we directly parameterize the inverse of  $R(x)$ , there is no matrix inversion when applying (10), making it more efficient for real-time application. The inverse formulation does not hinder the learning stage, as both  $R(x)$  and its inversion are always needed according to (12) and (13).

Figure 2 summarizes our algorithm, including matrix NN training and the design of stabilizing feedback control. Algorithm 1 provides the pseudocode of the learning process.

**Algorithm 1:** Learning Dissipativity of VSG-Based Power System With Stability Conditions

```

Input: data set  $\mathcal{D} = \{(x_k, x_{k+1}, u_k)\}_{k=1}^M$ ,  

       hyperparameters (number of epochs  $N_e$ , batch  

       size  $|\mathcal{B}|$ , size of MLP, learning rate, etc.)  

Output: Storage function  $V(x)$ , supply rate function  

        $w(x, u)$ , and stabilizing control  $\pi(x)$   

Initialize: Parameters  $\theta$  of  $W(x)$ ,  $Q(x)$ ,  $S(x)$ ,  $R(x)$   

for epoch = 0, 1, ...,  $N$  do  

  Randomly shuffle the data set  $\mathcal{D}$   

  Divide  $\mathcal{D}$  into batches of size  $|\mathcal{B}|$   

  for batch  $\mathcal{B}$  in batches do  

    Calculate loss  $\mathcal{L}(\theta, \mathcal{B})$  and  $\nabla_\theta \mathcal{L}(\theta, \mathcal{B})$   

    Update  $\theta$  with Adam optimizer  

return Control  $\pi(x) = -R^{-1}(x)S^T(x)x$ 

```

#### IV. SIMULATION VALIDATION

In this section, we validate our approach using numerical experiments of an SCIB system and a modified Kundur two-area system. In both cases, the nominal frequency is 60 Hz. Both post-fault systems had a stable equilibrium, but the fault-clearing states lay outside the corresponding RoAs. We used GELU (Gaussian-error linear unit) as the activation function and 128 as the output dimension of all hidden layers in every

MLP. We set the cost shaping goal as a quadratic cost  $l(x, u) = 1000\|\Delta\omega\|^2 + \|\Delta\delta\|^2 + 10\|u\|^2$ , where  $\|\cdot\|$  is the 2-norm,  $\Delta\omega$  and  $\Delta\delta$  are the frequency deviations and (relative) power angle deviations with respect to the post-fault equilibrium, and  $u$  are the control inputs. While we used higher-order dynamics of VSGs in the simulation, in the learning stage of our algorithm, we only considered second-order dynamics (1) (with unknown parameters), which is usually a sufficient representation of the higher-order system and helps reduce the computation effort. More specifically, we only used  $\Delta\omega$  and  $\Delta\delta$  as inputs to the NNs and to the generated controller.

##### A. Single Converter Infinite Bus System

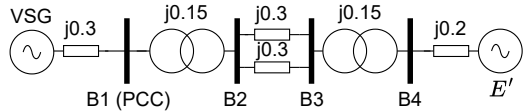


Fig. 3. Schematic of the SCIB system.

As seen in Figure 3, we considered a second-order VSG connected to an SG. The inertia of the SG was set to infinite, so the constant internal electromotive force  $E'$  acted as an (internal) infinite bus. The virtual inertia of the VSG was 4s, the damping coefficient was 5p.u., and the virtual impedance between the virtual electromotive force and the point of common coupling (PCC) was  $j0.3$ p.u. The system was initially set with nominal voltage at B1 and B4, and the voltage of B1 lagged behind B4 0.3rad;  $E'$  and the power set point of VSG were determined accordingly.

To train the matrix NNs, we first generated a data set containing  $(x_k, x_{k+1}, u_k)$  tuples with fixed sampling and control interval  $\Delta t = 0.5$  ms. As the convergence of post-fault states is decided by the post-fault dynamics, the training data were gathered in the post-fault system, which matched Figure 3 but with one line between B2 and B3 open, as described below.

To ensure sufficient excitation, we randomly sampled  $u_k$  and initial conditions from uniform distributions. We generated 2000 short trajectories of length 1s. After simulation, we filtered the sampled data to obtain a training data set that consisted only of data in a region of interest  $\tilde{\mathcal{X}}$  where  $|\Delta\omega| \leq 0.1$  and  $|\Delta\delta| \leq \pi$ . The filtering process ensures that the training focuses on a typical operating region of the system and helps

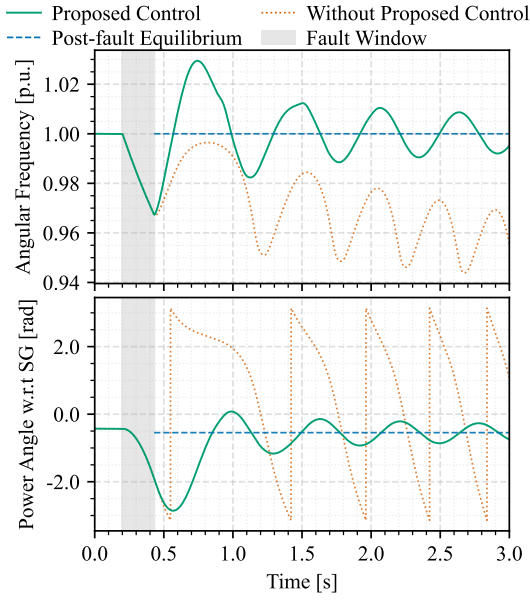


Fig. 4. The effect of proposed control in the SCIB system.

prevent unrealistic far-from-equilibrium data from distorting the gradients. We used a learning rate of  $5 \times 10^{-4}$  and weight decay  $10^{-4}$  in Adam,  $(w_1, w_2, w_3, w_4) = (10, 5, 0.1, 0.001)$ , and trained for 20 epochs.

To test the controller, the system was initialized at equilibrium and at  $t = 0.2$ s a three-phase ground fault occurred at B2. After 0.23s the fault was removed and one line between B2 and B3 was tripped as a protection mechanism. As shown in Figure 4, the converter frequency dropped and oscillated drastically in the post-fault stage without the proposed control, losing synchronization with the infinite bus, while the dissipativity-based control stabilized the power angle dynamics of the VSG, indicating an enlarged RoA of the post-fault equilibrium.

#### B. Kundur Two-Area System

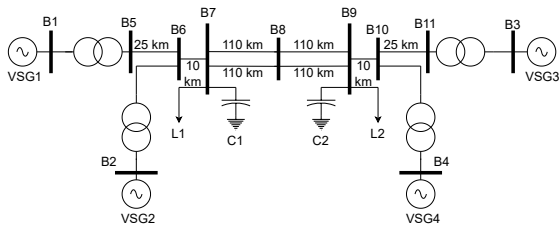


Fig. 5. The modified Kundur two-area system with VSGs.

We also tested our approach on the Kundur two-area system [9] modified to include four VSGs shown in Figure 5. The power and voltage set points of VSGs were the same as in the original Kundur system. The virtual impedance of each VSG was  $j0.3$ p.u., the virtual inertia was 4s, and the damping coefficient was 5p.u. To obtain isolated equilibrium points, we used power angles with respect to VSG1 and the angular frequencies as states.

To train the matrix NNs, we first used the same random sampling method as in the SCIB case to generate 2500 trajectories

of 1s with sampling and control interval of  $\Delta t = 0.5$ ms. The trajectories were gathered in the post fault system, where one line between B8 and B9 in Figure 5 was open. Next, we filtered the data and kept those belong to a region of interest  $\tilde{\mathcal{X}}$  satisfying  $\|\Delta\omega\|_\infty \leq 0.1$  and  $\|\Delta\delta\|_\infty \leq 2\pi$ , where  $\|\cdot\|_\infty$  is the infinity norm. Then we used a learning rate of  $10^{-3}$  and weight decay  $10^{-4}$  in Adam,  $(w_1, w_2, w_3, w_4) = (1, 1, 0.1, 10^{-3})$ , and trained for 20 epochs.

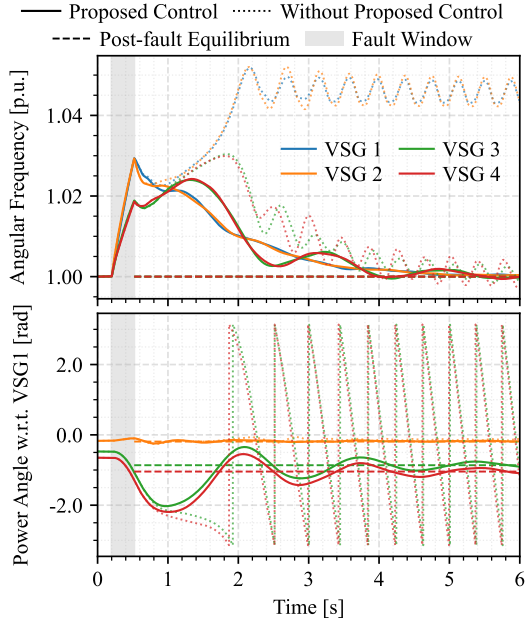


Fig. 6. The effect of proposed control in the two-area system.

To test the controller, we initiated the system at equilibrium and set a three-phase ground fault at  $t = 0.2$ s on one circuit between B8 and B9 near B8. After 0.32s the fault line was removed and necessary adjustments were made to the power and inner-loop set points of the VSGs to render a post-fault equilibrium with nominal frequency possible. Figure 6 shows that without the proposed control, VSG3 and VSG4 failed to synchronize with the other area with VSG1 and VSG2, and the frequency of each VSG fluctuated greatly, while the dissipativity-based neural control stabilized the VSG-based system in the post-fault stage, suggesting an enlarged RoA of the post-fault equilibrium.

## V. CONCLUSIONS

We propose a novel data-driven method for designing stabilizing controls for VSG-based power systems with unknown dynamics. The method utilizes neural networks to learn matrices that characterize the dissipativity of the unknown system while including stability conditions by penalizing violations of them. In consequence, the matrix NNs can synthesize a stabilizing feedback control with a dynamic gain. With extra degrees of freedom, the method can also integrate cost function shaping to enhance the optimality of the controller with respect to user-defined objectives. Numerical experiments on the transient stability of VSG-based power systems demonstrate the effectiveness of our algorithm. The proposed method is

expected to be extended to other stability problems of the modern power system, providing a valuable direction for future research.

## APPENDIX A PROOF OF THEOREM 2

**Proof:** When the control input  $u$  in (8) is given by the control law (10), the dissipativity condition (5b) implies

$$V(x_{k+1}) - V(x_k) \leq -x_k^T \Delta(x_k) x_k < 0, \forall x_k \in \mathcal{X}/\{0\},$$

where we have used condition (9) to rewrite the supply rate under the feedback (10).

Since  $V(x)$  is positive definite, it becomes a Lyapunov function as (4) requires. Thus,  $\pi(x)$  is a stabilizing control.  $\square$

## APPENDIX B PROOF OF THEOREM 3

**Proof:** According to Theorem 2, the asymptotical stability condition is satisfied. Condition (5b) implies that  $\tilde{l}(x_k, u_k)$  is nonnegative, while condition (9) indicates the positive definiteness of  $x_k^T \Delta(x_k) x_k$ . Consider the optimal cost:

$$\begin{aligned} J &= \min_{\{u_k\}_{k=0}^{\infty}} \sum_{k=0}^{\infty} [\tilde{l}(x_k, u_k) + x_k^T \Delta(x_k) x_k + u_k^T R(x_k) u_k] \\ &= - \sum_{k=0}^{\infty} [V(x_{k+1}) - V(x_k)] \\ &\quad + \min_{\{u_k\}_{k=0}^{\infty}} \sum_{k=0}^{\infty} [w(x_k, u_k) + x_k^T \Delta(x_k) x_k]. \end{aligned}$$

As (10) is a stabilizing control, the first summation reduces to  $-\sum_{k=0}^{\infty} [V(x_{k+1}) - V(x_k)] = V(x_0) - \lim_{k \rightarrow \infty} V(x_k) = V(x_0)$ . In the second summation, for each fixed  $x_k$ ,  $w(x_k, u_k)$  is quadratic in  $u_k$ . Since the quadratic coefficient  $R(x_k)$  is positive definite,  $w(x_k, u_k)$  attains its minimum value  $-x_k^T \Delta(x_k) x_k$  when  $u_k$  follows the feedback law (10). Therefore, the second summation  $\sum_{k=0}^{\infty} [w(x_k, u_k) + x_k^T \Delta(x_k) x_k]$  attains its minimum 0 under the same feedback law. In conclusion, the control law (10) is optimal with the respective minimal cost  $J = V(x_0)$ .  $\square$

## REFERENCES

- [1] F. Milano, F. Dörfler, G. Hug, D. J. Hill, and G. Verbić, “Foundations and challenges of low-inertia systems,” in *2018 power systems computation conference (PSCC)*. IEEE, 2018, pp. 1–25.
- [2] M. Chen, D. Zhou, and F. Blaabjerg, “Modelling, implementation, and assessment of virtual synchronous generator in power systems,” *Journal of Modern Power Systems and Clean Energy*, vol. 8, no. 3, pp. 399–411, 2020.
- [3] L. Harnefors, “Analysis of subsynchronous torsional interaction with power electronic converters,” *IEEE Transactions on power systems*, vol. 22, no. 1, pp. 305–313, 2007.
- [4] J. Fang, Y. Tang, H. Li, and F. Blaabjerg, “The role of power electronics in future low inertia power systems,” in *2018 IEEE International Power Electronics and Application Conference and Exposition (PEAC)*. IEEE, 2018, pp. 1–6.
- [5] M. Lu, S. Dutta, V. Purba, S. Dhople, and B. Johnson, “A grid-compatible virtual oscillator controller: Analysis and design,” in *2019 IEEE Energy Conversion Congress and Exposition (ECCE)*. IEEE, 2019, pp. 2643–2649.
- [6] P. Wang, J. Ma, R. Zhang, S. Wang, T. Liu, Z. Wu, and R. Wang, “Power self-synchronization control of grid-forming voltage-source converters against a wide range of short-circuit ratio,” *IEEE Transactions on Power Electronics*, vol. 38, no. 12, pp. 15419–15432, 2023.
- [7] X. He, M. A. Desai, L. Huang, and F. Dörfler, “Cross-forming control and fault current limiting for grid-forming inverters,” *IEEE Transactions on Power Electronics*, 2024.
- [8] R. Leng, L. Huang, H. Xin, P. Ju, X. Wang, E. Prieto-Araujo, and F. Dörfler, “DeePConverter: A data-driven optimal control architecture for grid-connected power converters,” *arXiv preprint arXiv:2508.08578*, 2025.
- [9] P. Kundur, N. J. Balu, and M. G. Lauby, *Power system stability and control*. McGraw-hill New York, 1994, vol. 7.
- [10] A. Pai, *Energy function analysis for power system stability*. Springer Science & Business Media, 1989.
- [11] M. Anghel, F. Milano, and A. Papachristodoulou, “Algorithmic construction of lyapunov functions for power system stability analysis,” *IEEE Transactions on Circuits and Systems I: Regular Papers*, vol. 60, no. 9, pp. 2533–2546, 2013.
- [12] W. Cui and B. Zhang, “Equilibrium-independent stability analysis for distribution systems with lossy transmission lines,” *IEEE Control Systems Letters*, vol. 6, pp. 3349–3354, 2022.
- [13] K. Urata and M. Inoue, “Dissipativity reinforcement in feedback systems and its application to expanding power systems,” *International Journal of Robust and Nonlinear Control*, vol. 28, no. 5, pp. 1528–1546, 2018.
- [14] P. Nahata, R. Soloperto, M. Tucci, A. Martinelli, and G. Ferrari-Trecate, “A passivity-based approach to voltage stabilization in DC microgrids with ZIP loads,” *Automatica*, vol. 113, p. 108770, 2020.
- [15] W. Cui, Y. Jiang, B. Zhang, and Y. Shi, “Structured neural-PI control with end-to-end stability and output tracking guarantees,” *Advances in Neural Information Processing Systems*, vol. 36, pp. 68434–68457, 2023.
- [16] D. J. Hill and T. Liu, “Dissipativity, stability, and connections: Progress in complexity,” *IEEE Control Systems Magazine*, vol. 42, no. 2, pp. 88–106, 2022.
- [17] A. Martinelli, A. Aboudonia, and J. Lygeros, “Interconnection of (Q, S, R)-dissipative systems in discrete time,” *arXiv preprint arXiv:2311.08088*, 2023.
- [18] T. Nakano, A. Aboudonia, J. Eising, A. Martinelli, F. Dörfler, and J. Lygeros, “Dissipativity-based data-driven decentralized control of interconnected systems,” *arXiv preprint arXiv:2509.14047*, 2025.
- [19] T. L. Vu and K. Turitsyn, “Lyapunov functions family approach to transient stability assessment,” *IEEE Transactions on Power Systems*, vol. 31, no. 2, pp. 1269–1277, 2015.
- [20] Y.-C. Chang, N. Roohi, and S. Gao, “Neural Lyapunov control,” *Advances in neural information processing systems*, vol. 32, 2019.
- [21] T. Zhao, J. Wang, X. Lu, and Y. Du, “Neural Lyapunov control for power system transient stability: A deep learning-based approach,” *IEEE Transactions on Power Systems*, vol. 37, no. 2, pp. 955–966, 2021.
- [22] T. Wang, X. Wang, G. Liu, Z. Wang, and Q. Xing, “Neural networks based Lyapunov functions for transient stability analysis and assessment of power systems,” *IEEE Transactions on Industry Applications*, vol. 59, no. 2, pp. 2626–2638, 2022.
- [23] R. Nelliikkath, I. Murzakhanov, S. Chatzivasileiadis, A. Venzke, and M. K. Bakhshizadeh, “Physics-informed neural networks for phase locked loop transient stability assessment,” *Electric Power Systems Research*, vol. 236, p. 110790, 2024.
- [24] R. Zhou, T. Quartz, H. De Sterck, and J. Liu, “Neural Lyapunov control of unknown nonlinear systems with stability guarantees,” *Advances in Neural Information Processing Systems*, vol. 35, pp. 29113–29125, 2022.
- [25] H. K. Khalil and J. W. Grizzle, *Nonlinear systems*. Prentice hall Upper Saddle River, NJ, 2002, vol. 3.
- [26] D. d. S. Madeira, “Necessary and sufficient dissipativity-based conditions for feedback stabilization,” *IEEE Transactions on Automatic Control*, vol. 67, no. 4, pp. 2100–2107, 2021.
- [27] T. A. Lima, D. d. S. Madeira, and M. Jungers, “QSR-dissipativity-based stabilization of non-passive nonlinear discrete-time systems by linear static output feedback,” *IEEE Control Systems Letters*, 2024.
- [28] H. Wang, K. Miao, D. Madeira, and A. Papachristodoulou, “Learning neural controllers with optimality and stability guarantees using input-output dissipativity,” *arXiv preprint arXiv:2506.06564*, 2025.
- [29] D. P. Kingma and J. Ba, “Adam: A method for stochastic optimization,” *arXiv preprint arXiv:1412.6980*, 2014.